



Synthesis of ultrafine gadolinium oxide powder by mechanochemical processing

Takuya Tsuzuki, William T.A. Harrison, Paul G. McCormick*

Special Research Centre for Advanced Mineral and Materials Processing, The University of Western Australia, Nedlands, Perth, WA 6907, Australia

Received 23 April 1998; received in revised form 14 August 1998

Abstract

The synthesis of ultrafine Gd_2O_3 powder by mechanochemical reaction and subsequent heat treatment via the reaction $2\text{GdCl}_3 + 3\text{CaO} \rightarrow \text{Gd}_2\text{O}_3 + 3\text{CaCl}_2$ was studied using X-ray diffraction, transmission electron microscopy and differential thermal analysis. Dried GdCl_3 and CaO powders were mechanically milled and subsequently annealed at various temperatures. During milling, GdOCl nanoparticles of ~ 16 nm in size were formed by a solid-state displacement reaction. Heat treatment of the as-milled powder at 700°C resulted in the formation of monoclinic Gd_2O_3 crystallites of ~ 100 nm having a thin platelet morphology. © 1998 Published by Elsevier Science S.A. All rights reserved.

Keywords: Gadolinium oxide; Ultrafine powder; Mechanochemical processing; Ball milling

1. Introduction

Recently gadolinium oxide (Gd_2O_3) has been investigated for a wide range of applications. It is used as a catalyst for dimerization of many organic compounds [1], a neutron converter in imaging plate neutron detectors [2], an additive in UO_2 fuel rods for nuclear reactors [3], an additive in ZrO_2 to enhance toughness [4], an additive in SiC and Si_3N_4 as a densification aid [5,6], and a dopant in CeO_2 fuel cells to enhance sintering properties [7]. Eu doped Gd_2O_3 is used for phosphors in ultraviolet detectors [8] and for scintillators coupled with a CCD TV camera for high resolution X-ray medical imaging [9]. For many of these applications, ultrafine Gd_2O_3 powder is the most desirable form.

Although many synthesis methods for rare earth oxides have been investigated [10,11], the synthesis of Gd_2O_3 is seldom encountered in the literature. The most common process is the thermal decomposition of precursors such as $\text{Gd}(\text{CH}_3\text{COO})_3 \cdot 4\text{H}_2\text{O}$ [1], $\text{Gd}(\text{OH})\text{CO}_3$ [12], and $\text{Gd}(\text{OH})_3$ [13,14]. However, the minimum particle size obtained with this method is limited by aggregation during thermal decomposition. Mazdiyasn et al. [13] have developed a dynamic calcination technique to prevent the aggregation during thermal decomposition of alkoxide

precursors, and have obtained Gd_2O_3 particles of ~ 28 nm in size. Rowley et al. [15] have synthesised a number of lanthanide oxides by a solid-state reaction of anhydrous lanthanide chloride and lithium oxide at 500°C . The reaction, however, yielded a fused lump of a mixture of lanthanide oxide, lanthanide oxy-chloride and lithium chloride.

Mechanochemical processing has been recently applied to the synthesis of a wide range of nanocrystalline materials [16,17]. Ding et al. [18–24] have reported the synthesis of nanoparticles of a number of transition metals and ceramics, such as Al_2O_3 , ZrO_2 , Fe_2O_3 and ZnS , by a novel method involving the mechanical activation of solid-state displacement reactions. Milling of precursor powders leads to the formation of a nanoscale composite structure of the starting materials which react during milling or subsequent heat treatment to form a mixture of separated nanocrystals of the desired phase within a soluble salt matrix. For example, ultrafine ZnS powder was synthesised by milling ZnCl_2 and CaS . The displacement reaction, $\text{ZnCl}_2 + \text{CaS} \rightarrow \text{ZnS} + \text{CaCl}_2$, was induced during ball milling, forming ZnS nanoparticles within a CaCl_2 matrix. Removal of the CaCl_2 by-product with a simple washing process resulted in separated ZnS particles of less than 10 nm in size [24]. This mechanochemical process is potentially applicable for the synthesis of Gd_2O_3 ultrafine particles via the reaction $2\text{GdCl}_3 + 3\text{CaO} \rightarrow \text{Gd}_2\text{O}_3 + 3\text{CaCl}_2$ because of the negative free energy change of -300

*Corresponding author. Tel.: +61-9-3803122; fax: +61-9-3801116; e-mail: pgm@shiralee.mech.uwa.edu.au

kJ mole^{-1} (100°C) [25]. In this paper, we report a study of the reaction between GdCl_3 and CaO during milling and subsequent heat treatment.

2. Experimental procedures

The starting materials were anhydrous GdCl_3 powder (Cerac, 99.9%, -20 mesh), CaO powder (Ajax, 98%, -100 mesh), and granular CaCl_2 (Aldrich, 97%). The GdCl_3 and CaCl_2 powders were dried under vacuum at 200°C , and CaO was calcined at 1000°C prior to use. The mixture of GdCl_3 and CaO powders with a stoichiometry of $2\text{GdCl}_3 + 3\text{CaO}$ was sealed in a hardened steel vial with steel balls of 12.7 mm in diameter, under a high-purity argon atmosphere. Milling was performed with a Spex 8000 mixer/mill using a ball to powder mass ratio of 40:1. The surface temperature of the vial was measured during milling using a thermocouple attached to the outside surface, in order to detect a possible combustion event. Removal of the CaCl_2 by-product was carried out by washing the powder with methanol, using an ultrasonic bath and a centrifuge. The washed powder was dried in an oven (60°C).

The structure of the powder was examined under an Ar-gas atmosphere with a Siemens D5000 X-ray diffractometer with $\text{Cu K}\alpha$ radiation at room temperature. The microstructure of the powder was studied using a Philips 430 transmission electron microscope (TEM) equipped with a Link energy-dispersive-spectroscopy (EDS) system. For TEM studies, the washed powder was dispersed in methanol using an ultrasonic bath and a drop of solution was placed on a copper grid coated with holey carbon film. Differential thermal analysis (DTA) was carried out using a Rigaku Thermoflex thermal analysis system under constant Ar-gas flow of 2 cc min^{-1} with a heating rate of $20^\circ\text{C min}^{-1}$. BET surface area was measured using a Micromeritics Gemini 2360 Surface Area Analyser by N_2 -gas adsorption at 77 K.

3. Results

No combustion was detected during milling of the $2\text{GdCl}_3 + 3\text{CaO}$ powder mixtures. In Fig. 1 the X-ray diffraction (XRD) patterns of the powder milled for different times are shown. After milling for 2 h, the peaks corresponding to GdCl_3 and CaO became weak and broad due to the development of a nanoscale composite mixture. Peaks corresponding to GdOCl appeared after milling for 4 h, and their intensity increased gradually with increasing milling time. After milling for 8 h, the diffraction pattern consisted of peaks associated with GdOCl and CaO . No change in the diffraction pattern was found after milling for longer than 8 h, indicating that the reaction $\text{GdCl}_3 + \text{CaO} \rightarrow \text{GdOCl} + \text{CaCl}_2$ has completed during milling for 8

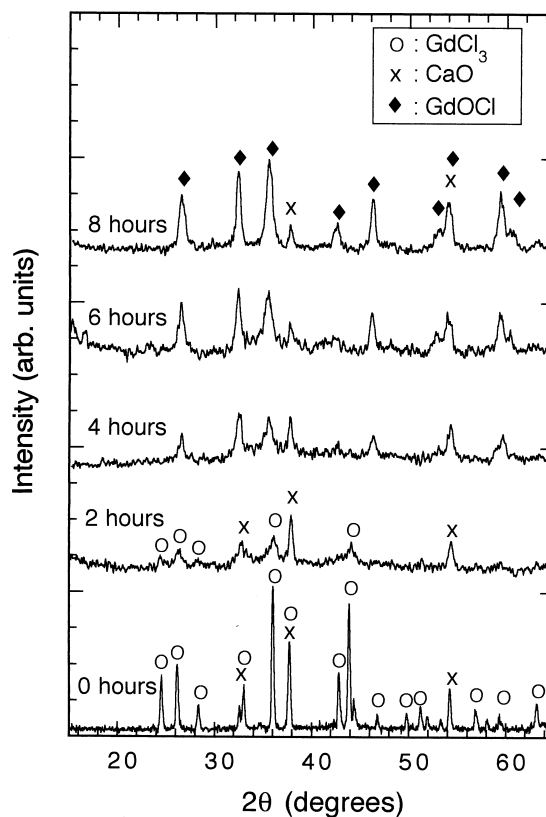


Fig. 1. X-ray diffraction patterns of $2\text{GdCl}_3 + 3\text{CaO}$ powder milled for different times.

h. The peaks corresponding to CaCl_2 were not evident in the XRD pattern, because the CaCl_2 by-product was amorphous [24]. Average particle sizes of GdOCl and CaO in the powder milled for 8 h were estimated from the XRD peak width using the Scherrer method [26] to be 16 and 24 nm, respectively.

In Fig. 2 a TEM micrograph of the powder milled for 8 h and subsequently washed to remove the CaCl_2 by-

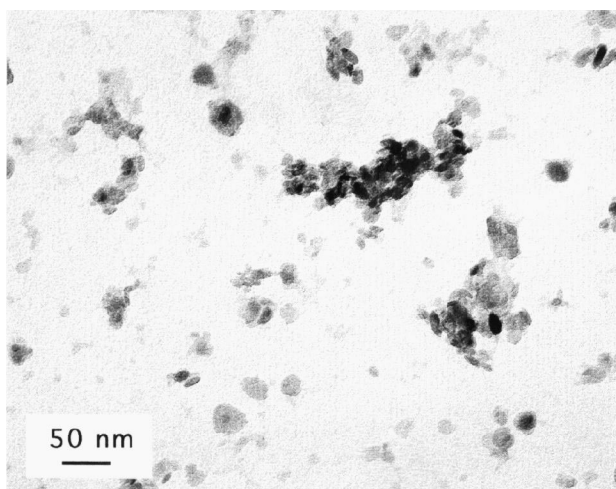


Fig. 2. Transmission electron micrograph of the $2\text{GdCl}_3 + 3\text{CaO}$ powder milled for 8 h and subsequently washed.

product is shown. A large number of free particles were evident, and some crystallites were loosely agglomerated. Using EDS and electron diffraction measurements, the particles were identified as GdOCl and CaO. The crystallites have sizes between 5 and 40 nm, which is consistent with XRD measurements.

The powder milled for 8 h was annealed at different temperatures in a sealed fused-silica tube under vacuum. In Fig. 3 the XRD patterns of the as-milled and subsequently annealed powders are shown. The XRD pattern of the sample annealed at 350°C for 1 h showed no change from that of the as-milled sample. In the pattern of the sample annealed at 600°C for 1 h, the peaks associated with CaO disappeared and Ca₄OCl₆ phase [27] appeared, as indicated with arrows. The position and width of the peaks corresponding to GdOCl remained unchanged up to this temperature. The Ca₄OCl₆ phase was formed between the residual CaO and the by-product CaCl₂ via the reaction $\text{CaO} + 3\text{CaCl}_2 \rightarrow \text{Ca}_4\text{OCl}_6$. Although other compounds between CaO and CaCl₂ such as Ca₃OCl₄ [28] and Ca₅OCl₈ [29] have been reported by thermal analysis, only the

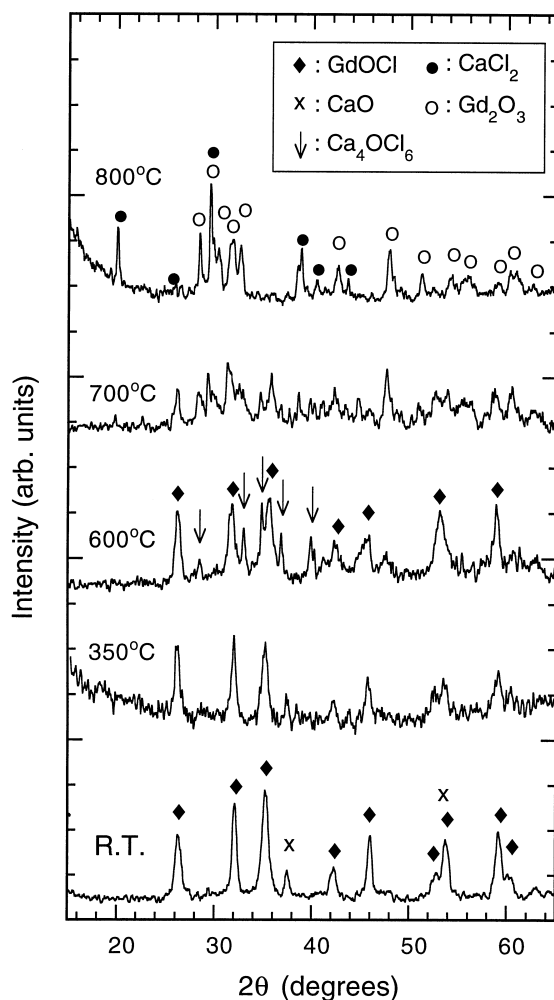


Fig. 3. X-ray diffraction patterns of the as-milled and subsequently annealed 2GdCl₃ + 3CaO powders at different temperatures for 1 h.

Ca₄OCl₆ phase was formed in this study. Annealing at 700°C for 1 h resulted in a complicated diffraction pattern consisting of the peaks associated with GdOCl, Gd₂O₃, and Ca₄OCl₆. After annealing at 800°C for 1 h, the pattern consisted of peaks corresponding to CaCl₂ and monoclinic Gd₂O₃, suggesting that the reaction to form Gd₂O₃ was completed.

In Fig. 4 the XRD patterns of the milled powder annealed at 700°C for different times are shown. As the annealing time increased, the peaks associated with GdOCl gradually weakened. The Gd₂O₃ peaks appeared after annealing for 1 h, and increased their intensity with annealing time. About 5 h was required to complete the reaction. After washing the sample annealed at 700°C for 5 h, only the peaks associated with Gd₂O₃ were evident as shown in Fig. 5.

In Fig. 6 the DTA curve of the powder milled for 8 h is shown. A small exothermic peak was evident around 420°C. An endothermic reaction started around 670°C, and a sharp peak appeared at 800°C. The onset temperature of the sharp peak was determined, as indicated in the figure with dotted lines and an arrow, to be 770°C, which is nearly the same as the melting point of bulk CaCl₂ (772°C). Since the peaks corresponding to Ca₄OCl₆ ap-

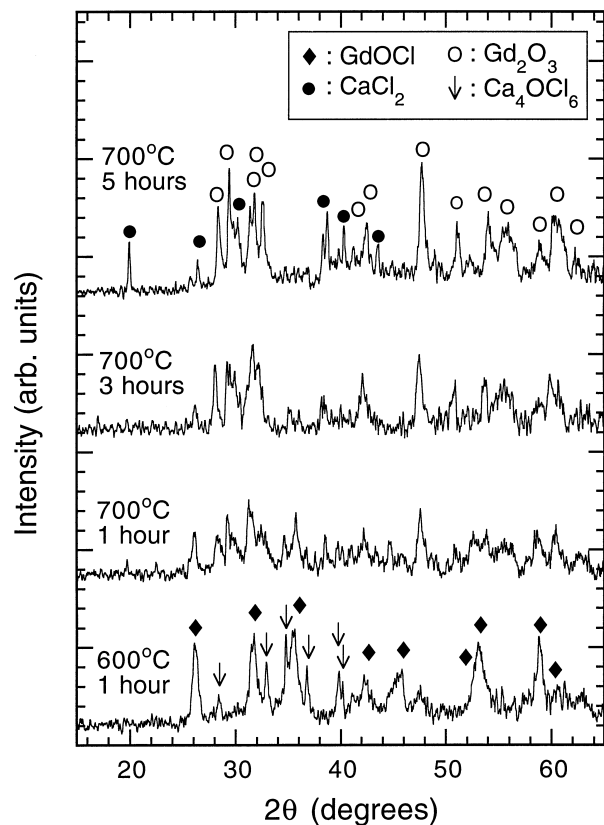


Fig. 4. X-ray diffraction patterns of the 2GdCl₃ + 3CaO powder milled for 8 h and subsequently annealed at 700°C for different times. Annealing time was indicated in the figure. The pattern of the powder annealed at 600°C was also shown for comparison.

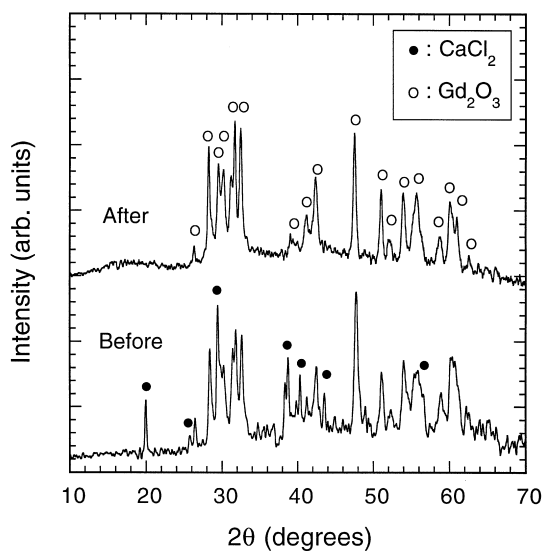


Fig. 5. X-ray diffraction patterns of the annealed powder before and after washing. The powder was annealed at 700°C for 5 h.

peared in the XRD pattern above 600°C (Fig. 3), the small exothermic peak at 420°C may be related to the formation of the Ca_4OCl_6 phase. The reaction to form Gd_2O_3 , which occurred above 700°C according to the XRD data, was not detected by the DTA measurement.

In Fig. 7(a) a TEM micrograph of the washed powder milled for 8 h and subsequently annealed at 700°C for 5 h is shown. The particles have geometrical thin plate shapes with sizes of 20–150 nm. No trace of Ca or Cl was detected by EDS. Using dark field imaging, the particles were found to be single crystals. The thickness of the platelets were 5–20 nm. The size distribution was not measured because of the irregular shapes of the platelets. Annealing at 800°C resulted in larger particles (Fig. 7(b)).

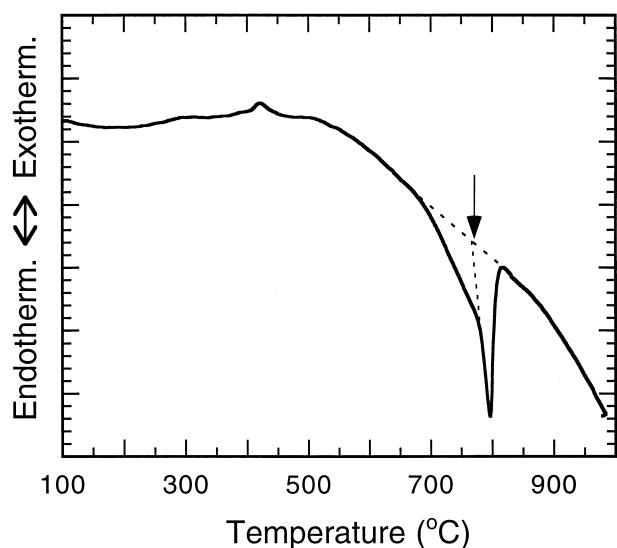
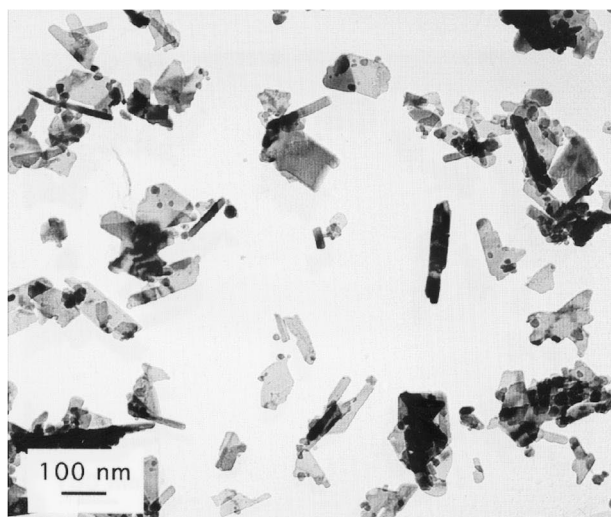
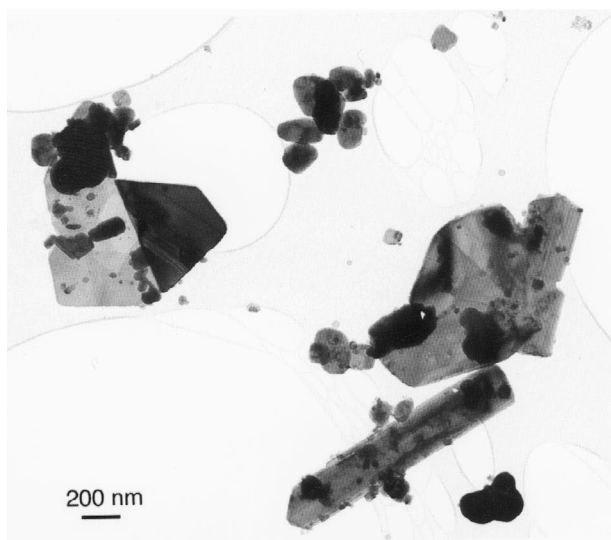


Fig. 6. Differential thermal analysis curve of the $2\text{GdCl}_3 + 3\text{CaO}$ powder milled for 8 h.



(a)



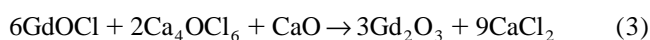
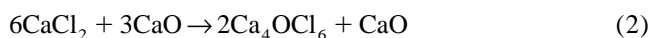
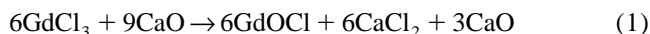
(b)

Fig. 7. Transmission electron micrographs of the washed Gd_2O_3 particles obtained by milling of $2\text{GdCl}_3 + 3\text{CaO}$ powder for 8 h and subsequently annealed at (a) 700°C for 5 h, and (b) 800°C for 1 h.

The powder annealed at 700°C had a BET surface area of $47.7 \text{ m}^2 \text{ g}^{-1}$.

4. Discussion

The present investigation has shown that the formation of Gd_2O_3 occurred in three separate stages:



As shown in Fig. 1, reaction 1 occurred after milling for 8 h. This is consistent with the fact that the free energy change in this reaction is negative ($-135 \text{ kJ mole}^{-1}$ at 100°C) [25]. With the starting stoichiometry used, the as-milled powder after the reaction should have consisted of GdOCl , CaO and CaCl_2 . Gd_2O_3 would normally be expected to be formed between GdOCl and residual CaO via the reaction $2\text{GdOCl} + \text{CaO} \rightarrow \text{Gd}_2\text{O}_3 + \text{CaCl}_2$, due to the negative free energy change of -27 kJ mole^{-1} (100°C) [25]. However, this reaction did not occur during milling, presumably because of slow reaction kinetics. It is of interest to note that free energy change in the reaction $2\text{LnOCl} + \text{CaO} \rightarrow \text{Ln}_2\text{O}_3 + \text{CaCl}_2$ ($\text{Ln} = \text{lanthanides}$) is positive for light-weight lanthanides such as La , Nd and Sm , while it is negative for Gd and the heavier lanthanides.

The platelet shape of Gd_2O_3 particles suggests that the crystallites grew in a liquid phase. For the sample milled for 8 h, the endothermic reaction started at 670°C (Fig. 3), which is lower than the heat treatment temperature of 700°C . Although this temperature is lower than the melting points of GdOCl , Ca_4OCl_6 and CaCl_2 , this endothermic reaction is likely to be due to the melting of GdOCl – Ca_4OCl_6 system, where the melting point is decreased due to the formation of a eutectic mixture [30].

For Gd_2O_3 , the cubic structure is thermodynamically stable below 1200°C . The Gd_2O_3 platelets obtained in this study, however, had the monoclinic high-temperature phase. Although the formation of plate-like particles in molten salts has been reported for other oxides such as $\text{Sr}(\text{Fe}_2\text{O}_3)_6$ [31], $\text{Ba}(\text{Fe}_2\text{O}_3)_6$ [32,33], BiWO_6 [34,35] and $\text{Bi}_4\text{Ti}_3\text{O}_{12}$ [36], the particles of these materials had thermodynamically stable phases. The mechanism of the formation of monoclinic platelets in the present study is yet unknown and is a subject of future studies.

Ceramic nanoparticles of $<10 \text{ nm}$ in size have recently been synthesised by various methods [10,11,37]. The sizes of Gd_2O_3 platelets obtained in the present study were as large as $\sim 100 \text{ nm}$. However, with the exception of the dynamic calcination technique of Mazdiyasnı et al. [13], the particle sizes of the powders synthesised in this study are significantly smaller than that of powders synthesised by the thermal decomposition methods commonly used for the synthesis of Gd_2O_3 powders [1,12,14,38–40].

5. Conclusions

This study has demonstrated the synthesis of ultrafine Gd_2O_3 particles from GdCl_3 and CaO powders by mechanochemical reaction and subsequent heat treatment. During the milling of powder having a stoichiometry of $2\text{GdCl}_3 + 3\text{CaO}$, a solid-state displacement reaction $\text{GdCl}_3 + \text{CaO} \rightarrow \text{GdOCl} + \text{CaCl}_2$ occurred in a steady-state manner, resulting in the formation of GdOCl particles with sizes less than 20 nm . During subsequent heat treatment at 700°C , unagglomerated metastable monoclinic Gd_2O_3

particles were formed in a CaCl_2 matrix via the reaction $6\text{GdOCl} + 2\text{Ca}_4\text{OCl}_6 + \text{CaO} \rightarrow 3\text{Gd}_2\text{O}_3 + 9\text{CaCl}_2$. Removal of the CaCl_2 by-product was carried out by dissolution in methanol. The Gd_2O_3 particles had irregular-shape plate-like morphology with length of 100 nm and thicknesses of $5\text{--}20 \text{ nm}$.

Acknowledgements

Authors would like to thank Mr Robert Skala for useful discussions about X-ray diffraction analysis.

References

- [1] G.A.M. Hussein, *J. Phys. Chem.* 98 (1994) 9657.
- [2] K. Takahashi, S. Tazaki, J. Miyahara, Y. Karasawa, N. Niimura, *Nucl. Instrum. Methods Phys. Res. A* 377 (1996) 119.
- [3] G. Gunduz, I. Uslu, *J. Nucl. Mater.* 231 (1996) 113.
- [4] S. Bhattacharyya, D.C. Agrawal, *J. Mater. Sci.* 30 (1995) 1495.
- [5] Z. Chen, *J. Am. Ceram. Soc.* 79 (1996) 530.
- [6] C.M. Wang, X. Pan, M.J. Hoffmann, R.M. Cannon, M. Ruehie, *J. Am. Ceram. Soc.* 79 (1996) 788.
- [7] E.O. Ahlgren, F.W. Poulsen, *J. Phys. Chem. Solids* 57 (1996) 589.
- [8] S.M. Yeh, C.S. Su, *Radiation Protection Dosimetry* 65 (1996) 359.
- [9] H.D. Zeman, F.A. Dibanca, G. Lovhoiden, *Proc. SPIE – Int. Soc. Opt. Eng.* 2432 (1995) 454.
- [10] G.-Y. Adachi, N. Imanaka, *Chem. Rev.* 98 (1998) 1479.
- [11] L. Eyring, *Synthesis of Lanthanide and Actinide Compound*, Kluwer Academic, Netherlands, 1991, p. 187.
- [12] E. Matijevic, W.P. Hsu, *J. Colloid Interface Sci.* 118 (1987) 506.
- [13] K.S. Mazdiyasnı, L.M. Brown, *J. Am. Ceram. Soc.* 54 (1971) 479.
- [14] F. Imoto, T. Nanatani, S. Kaneko, *Ceram. Trans.* 1 (1988) 204.
- [15] A.T. Rowley, I.P. Parkin, *Inorg. Chim. Acta* 211 (1993) 77.
- [16] P.G. McCormick, J. Ding, H. Yang, T. Tsuzuki, *Materials Research* 96, vol. 1, IMMA, 1996, p. 85.
- [17] G.B. Schaffer, P.G. McCormick, *Mater. Forum* 16 (1992) 91.
- [18] J. Ding, W.F. Miao, P.G. McCormick, R. Street, *Appl. Phys. Lett.* 67 (1995) 3804.
- [19] J. Ding, T. Tsuzuki, P.G. McCormick, R. Street, *J. Alloys Comp.* 234 (1996) L1.
- [20] J. Ding, T. Tsuzuki, P.G. McCormick, R. Street, *J. Phys. D: Appl. Phys.* 29 (1996) 2365.
- [21] J. Ding, T. Tsuzuki, P.G. McCormick, *J. Am. Ceram. Soc.* 79 (1996) 2956.
- [22] J. Ding, T. Tsuzuki, P.G. McCormick, *Nanostruct. Mat.* 8 (1997) 75.
- [23] J. Ding, T. Tsuzuki, P.G. McCormick, *Nanostruct. Mat.* 8 (1997) 739.
- [24] T. Tsuzuki, J. Ding, P.G. McCormick, *Physica B* 239 (1997) 378.
- [25] I. Barin, *Thermochemical Data of Pure Substances*, VCH, Weinheim, 1989.
- [26] B. Cullity, *Elements of X-ray diffraction*, 2nd ed., Addison-Wesley, Redding, 1978.
- [27] H.-J. Meyer, G. Meyer, M. Simon, *Z. Anorg. Allg. Chem.* 596 (1991) 89.
- [28] B. Neumann, C. Krocger, H. Juettner, *Z. Electrochem.* 41 (1935) 725.
- [29] I. Poletaev, A.P. Lyudomirskaya, A.I. Ismailov, N.D. Tsildina, *Russ. J. Inorg. Chem.* 21 (1976) 1256.
- [30] P.G. Permyakov, B.G. Korshunov, V.A. Krokhnin, *Russ. J. Inorg. Chem.* 19 (1974) 1739.

- [31] N. Horiishim, S. Yamamoto, Proceedings of the 6th International Conference on Ferrites, Tokyo, 1992, p. 1041.
- [32] K.H. Yoon, D.H. Lee, H.J. Jung, S.O. Yoon, *J. Mater. Sci.* 27 (1992) 2941.
- [33] J. Ding, T. Tsuzuki, P.G. McCormick, *J. Magn. Magn. Mater.* 177(part 2) (1998) 931.
- [34] T. Kimura, M.H. Holmes, R.E. Newnham, *J. Am. Ceram. Soc.* 65 (1982) 223.
- [35] F. Soares-Carvalho, J.-H. Yi, M. Manier, P. Thomas, J.-P. Mercurio, B. Frit, *Key Eng. Mater.* 132–136 (1997) 34.
- [36] H. Watanabe, T. Kimura, T. Yamaguchi, *J. Am. Ceram. Soc.* 72 (1989) 289.
- [37] R. Freer, ed., *Nanoceramics*, British Ceramics Proceedings 51, Institute of Materials, London, 1993.
- [38] T.V. Mani, H.K. Varma, A.D. Damodaran, K.G.K. Warner, *Ceram. Int.* 19 (1993) 125.
- [39] M.I. Levin, E.A. Bondarenko, N.L. Nazarova, S.S. Kulagina, E.E. Belousova, *Sov. J. Opt. Technol.* 58 (1991) 118.
- [40] H.K. Varma, P. Mukundan, K.G.K. Warier, A.D. Damodaran, *J. Mater. Sci. Lett.* 9 (1990) 377.